SYNTHESIS OF FLUORAPATITE NANOPOWDERS BY A SURFACTANT-ASSISTED MICROWAVE METHOD UNDER ISOTHERMAL CONDITIONS

by

Vojislav Dj. STANIĆ [1*], ***Borivoj K. ADNADJEVIĆ*** [2], ***Suzana I. DIMITRIJEVIĆ*** [3], ***Slavko D. DIMOVIĆ*** [1], ***Miodrag N. MITRIĆ*** [1], ***Bojana B. ZMEJKOVSKI*** [4], ***and Slavko SMILJANIĆ*** [5]

[1] Vinča Institute of Nuclear Sciences, University of Belgrade, Belgrade, Serbia
[2] Faculty of Physical Chemistry, University of Belgrade, Belgrade, Serbia
[3] Faculty of Technology and Metallurgy, University of Belgrade, Belgrade, Serbia
[4] Department of Chemistry, Institute of Chemistry, Technology and Metallurgy, University of Belgrade, Belgrade, Serbia
[5] Faculty of Technology, University of East Sarajevo, Republic of Srpska, Bosnia and Herzegovina

Scientific paper
http://doi.org/10.2298/NTRP1802180S

Fluorapatite nanopowders with different amounts of fluoride ions were prepared using the surfactant-assisted microwave method under isothermal conditions. Microwave irradiation was applied for the rapid formation of crystals. A micellar solution of polyoxyethylene (23) lauryl ether was used as a regulator of nucleation and crystal growth. Characterization studies from X-ray diffraction, field-emission scaning electron microscopy and Fourier-transform infrared spectra showed that crystals have an apatite structure and particles of all samples are nano size, with an average length of 50 nm and about 15-25 nm in diameter. Antimicrobial studies have demonstrated that synthesized fluorapatite nanopowders exhibit activity against tested pathogens: *Escherichia coli, Staphylococcus aureus* and *Candida albicans*. Activity increased with the amount of fluoride ions. The synthesized fluorapatite nanomaterials are promising as materials in environmental protection and medicine for orthopedics and dental restorations.

Key words: fluorapatite, microwave processing, nanopowder, environmental protection

INTRODUCTION

Synthetic apatite materials have been an indispensable component of various applications in environmental protection and medicine for orthopedics and dental restorations [1-3]. The toxic and radioactive heavy metals are one of the most dangerous toxic contaminants in the environment, especially in ground water and soil. The fate of heavy metals in the environment depends mainly on their interaction with minerals. The stability of the final product of this interaction represents a key factor, which determines mobility and biological availability of heavy metal pollutants in the environment. Apatite was selected as an ideal material for long-term containment of heavy metals, which have a high sorption capacity for these metals, low water solubility, high stability under reducing and oxidizing conditions, low cost, and availability. The apatites investigated include synthetic hydroxyapatite (HAP; $Ca_{10}(PO_4)_6(OH)_2$) and fluoroapatite (FAP; $Ca_{10}(PO_4)_6F_2$), apatites of biological origin and naturally occurring apatite minerals [4-7]. Fluoroapatite, in comparison to pure hydroxyapatite and other apatite materials, has higher physico-chemical stability, such as an increased resistance to dissolution by acid [8]. It has a high affinity for uranium and other radionuclides [9]. Alpha radiation, resulting from the decay of radionuclides, found in the crystalline structure of apatite materials can induce crystalline to amorphous transformation [10-12]. Fluorapatite materials showed radiation-damage resistance at temperatures above 70 °C, making them very promising materials for nuclear waste storage [13]. Biomaterials based on fluoroapatite have been very promising because of their crystallographic similarities to the natural inorganic component of bone (hydroxyapatite). *In vitro* and *in vivo* studies have shown that synthetic fluoroapatite is a possible replacement for bone repair due to its biocompatibility, bioactivity, and osteo- conductive properties [14]. Implant-associated infections present significant surgical

* Corresponding author; e-mail: voyo@vin.bg.ac.rs

problems and usually require removal [15]. To solve the problem of implant related infections, the use of bone implants which include antimicrobial agents such as antibiotics, fluoride and biocides metal ions is proposed [16-18]. Fluoride ions play an important role in the prevention and control of dental caries. Fluorapatite materials showed potential antibacterial activity but not the biocidal effect [16].

The many applications of fluoroapatite materials mainly depend on the chemical composition, shape, morphology, and size of apatite particles. Therefore, various synthesis methods of fluorapatite have been developed in recent years: neutralization [16], sol-gel [19], surfactant-assisted [20], mechanochemical synthesis [21], microwave [22] and flame spray pyrolysis [23]. Most of these methods require time consuming procedures and obtain macroscopic particles.

Microwave heating is a widely accepted, non-conventional energy source for inorganic, organic synthesis, and different physicochemical processes, such as sintering, nucleation and crystallization, adsorption, and so forth [24, 25]. The effect of microwave irradiation on the kinetics of chemical reactions is explained by thermal effects, such as overheating, hot-spots, selective heating or as a consequence of specific microwave effects. The main advantages of using the microwave method, relative to conventional heating methods in chemical synthesis, are rapid volumetric heating, higher reaction rate, shorter reaction time, selectivity, and higher yield. The surfactant-assisted method is very promising for synthesis of apatite nanoparticles [20]. Surfactant properties, in particular the polarity of the heads as well as its quantity in the solution, can affect the crystallization process, the chemical composition, size and morphology of apatite particles. Several studies have shown that surfactants have an impact on the morphology and size of apatite particles obtained by the microwave method [26, 27]. Gopi *et al*. [26] reported the synthesis of hydro- xyapatite nanospheres by using the microwave heating method and hexadecyltrimethylammonium bromide (CTAB) as a template. Arami *et al*. [27] reported the synthesis of hydroxyapatite nanostrips with an average width of 10 nm and length of 55 nm using CTAB as the surfactant.

In this work, fluorapatite ($Ca_{10}(PO_4)_6F_x(OH)_{2-x}$, 0 x 2) powders with different fluoride concentrations were synthesized by the surfactant-assisted microwave method. The main reason for using the surfactant-assisted microwave method is the possibility of preparing nanoproducts in a short time from relatively inexpensive chemicals, and thereby making it suitable for an industrial production. The antimicrobial activity of fluorapatite samples was tested against different pathogens: *Staphylococcus aureus (S. aureus), Escherichia coli (E. coli)*, and *Candida albicans (C. albicans)* was evaluated *in vitro*.

MATERIALS AND METHODS

Preparation of the materials

The starting materials were $Ca(CH_3COO)_2xH_2O$ (AppliChem), $(NH_4)_2HPO_4$ (Merck), polyoxyethylene (23) lauryl(ether) (Brij 35; Alfa Aesar), NaF (VWR) and NH4OH (Merck) of pro analysis grade of purity. The microwave assisted reactions were conducted using a microwave reactor (Discover, CEM Corp., Matthews, N. C., USA) supplied with a programmed temperature control system. All the reactions were carried out in the microwave field of 2.45 GHz, maintaining the desired temperatures at 60 °C.

The first solution was prepared by mixing 50 mL of 0.1 M Brij 35 and 100 mL of $Ca(CH_3COO)_2$ (0.11 M). The second solution of 50 mL $(NH_4)_2HPO_4$ (0.13 M) and NaF (0.01 M; 0,.02 M; 0.03 M or 0.04 M) was dropped into the first solution. The pH of both solutions was maintained at 10 by the NH_4OH solution before mixing. The synthesis process in a microwave field lasted 15 minutes with constant stirring. The precipitate thus obtained was filtered by a vacuum filtration process. The precipitate was washed with ethanol and water to remove the excess of Brij 35, and dried at 105 ºC and pulverized into a powder.

Characterization of synthesized apatite samples

The X-ray diffraction (XRD) studies of the apatites were performed using a Philips PW 1050 diffractometer, using CuK1.2 Ni-filtered radiation. The diffracted X-rays were collected over a 2θ range 20-80° using a step width of 0.02° and measured for 1 s per step. Lattice parameters *a*, *b*, and *c* of the apatite hexagonal unit cell and average crystallite size were determined using the Powder Cell 2.4 program.

The Fourier-transform infrared (FTIR) spectra of synthesized apatite samples, were recorded on a Nicolet 6700 FTIR spectrophotometer (Thermo Scientific) using the ATR technique, in a frequency interval of 4000-400 cm^{-1}.

The morphology of the obtained powders was studied by field-emission scanning electron microscopy (FESEM) TESCAN Mira3 XMU at 20 kV. Prior to the SEM analysis, the powder samples were coated with an Au-Pd alloy using a spatter coater.

The semi-quantitative chemical analysis of the samples was analysed using an energy dispersive spectrometer (EDS) with a SiLi X-ray detector (Oxford Instruments, UK) connected to a scanning electron microscope and a computer multi-channel analyzer. The measurements were performed to detect calcium, phosphorus, and fluor.

The combined measurements uncertainty of the experimental procedures was less than 5 % [28-30].

In vitro antimicrobial activity

Antimicrobial activities of samples were investigated, by a modified liquid challenge method, [31] against a gram-negative bacterial strain *E. coli* (ATCC 25922), gram-positive bacterium *S. aureus* (ATCC 25923) and yeast *C. albicans* (ATCC 24433). Prior to obtaining inoculum, bacteria were cultivated on nutrition agar No. 8 and yeast on malt extract agar No. 37 slants (LabM, U. K). The incubation time for bacteria was 24 h at 37 °C and for yeast 48 h at 28 °C.

The 0.01 g of an appropriate apatite sample was challenged to 1 mL of an inoculated buffered saline solution containing about 2.1 10^6 cfumL^{-1} (*S. aureus*), 7.54 10^6 cfumL^{-1} (*E. Coli*) and 2 10^6 cfumL^{-1} (*C. albicans*). After one hour of incubation at 37 °C in a water bath shaker, 9 mL of saline was added and the suspension was vigorously vortexed for 3 min to separate the cells since they tend to adsorb to the particles [16]. Aliquots of 1 mL were taken as samples for further dilution with saline and viable cell determination by seeding in agar plate Petri dishes with a corresponding medium. The formed colony units were counted after incubation in a thermostat under appropriate conditions.

The percentage of viable cell reduction (R %) was calculated using the eq. (1).

$$R[\%] \quad 100\ (C_0 \quad C)/C_0 \qquad (1)$$

where C_0 is the average number of strain colonies of the control, and C – the corresponding number of colonies of challenged apatite samples at the same predetermined time.

RESULTS

Characterization of apatite nanocrystals

The XRD patterns of synthesized apatite samples are presented in fig. 1. The positions of its X-ray diffraction peaks were in accordance with ASTM data for hydroxyapatite (Card 9-0432) and fluorapatite (Card 15-0876). The lattice parameters, crystallite size and the fraction of the crystalline phase of all samples are presented in tab. 1.

The results of EDS analysis for calcium, phosphorus, and fluor of all samples are shown in tab. 2.

The FTIR spectra of the samples are shown in fig. 2. The spectra show the characteristic bands for phosphate and hydroxyl groups and absorbed water. The dominant bands that appear at 1043-1018 cm^{-1} and the small band at 961 cm^{-1} belong to the asymmetric stretch vibration of PO_4^3 groups, while the bands at 563-550 cm^{-1} originate from the stretching symmetric vibrations. The bands at 451-432 cm^{-1} correspond to a symmetrical vibration from PO_4^3 groups. The

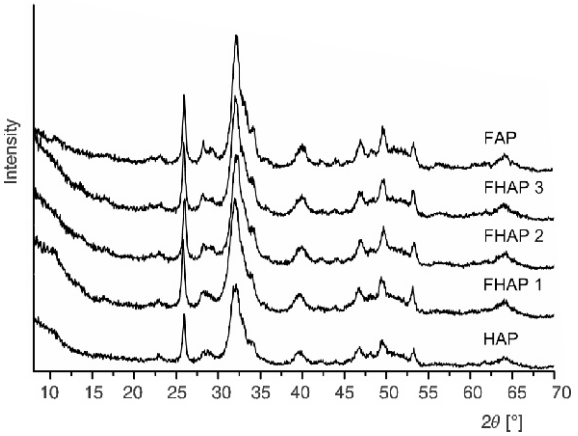

Figure. 1 XRD patterns of hydroxyapatite and fluorapatites with different contents of fluoride ions

Table 1. Unit cell parameters and crystallite sizes (Xs) of all synthesized apatite samples

Sample	a	c	Xs
HAP	9.43484	6.88009	17.5
FHAP1	9.42393	6.88472	13.5
FHAP2	9.39608	6.88162	15.7
FHAP3	9.38626	6.88482	17.5
FAP	9.38450	6.88427	19.9

Table 2. The results of EDS analyses of hydroxyapatite and fluorapatite samples (*atomic ratio [%])

Sample	Ca*	P*	Ca/P		F*
			Nominal	Measured	
HAP	14.84	9.76	1.67	1.52	0
HFAP1	15.87	9.44	1.67	1.68	0.53
FHAP2	15.76	9.22	1.67	1.71	1.84
FHAP3	17.21	9.88	1.67	1.74	2.80
FAP	18.29	9.66	1.67	1.89	3.10

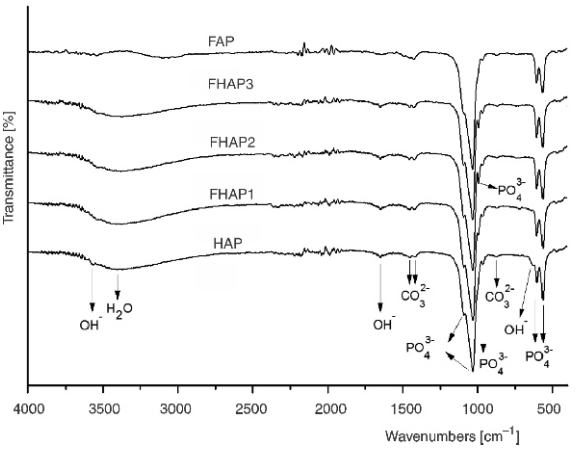

Figure 2. FTIR transmittance spectra of synthesized samples: hydroxyapatite and fluorapatites with different content of fluoride ions

FHAP1, FHAP2, and FHAP3 samples contain an additional band originating from the PO_4^3 groups at about 991 cm^{-1}. The weak bands at about 1430 cm^{-1} and 870 cm^{-1} indicate the presence of carbonate ions in samples. The broad absorption band at 2500-3700 cm^{-1} and weak at 1640 cm^{-1} are assigned to the adsorbed water. The weak band of the hydroxyl group located approximately at 3572 cm^{-1} is easily visible in the HAP sample. FESEM micrographs of the HAP and FHAP samples are presented in fig. 3. Morphology of the synthesized samples were was similar. The particles have a nano-size character and an irregular rod-like morphology. The average lenghtlength of particles in all samples is about 50 nm in lenghtlength and they have are about 15-25 nm in diameter.

The results of antimicrobial activity determination

The results of the antimicrobial tests of the fluorapatite samples against microbes are shown in fig. 4. The antimicrobial effect demonstrates that all apatite samples show viable cell reduction of microbial species. Antimicrobial activity of fluorapatite materials is a function of quantities of fluoride ions and the types of microbes.

DISCUSSION

One of the most promising methods for the synthesis of apatite materials is the microwave method. Microwave radiation creates a heating solution which can affect the stability of the surfactant micellar solution. In this work isothermal conditions ($T = 60$ ºC) are used to ensure the stability of the micellar solutions. The used concentration of Brij 35 (0.025 M) is higher than the critical micellar concentration (CMC) of 0.048 mM at 25 ºC and 0.034 mM at 50 ºC [32, 33]. Schwarzenbacher *et al*. [34] reported that an aqueous solution of Brij 35 (to 30 % w/w) at 60 ºC is micellar while at higher ratios leads to the formation of an isotropic surfactant liquid.

The XRD patterns (fig. 1) of synthesized samples are similar, diffraction peaks were broad, indicating that the obtained products have low crystallinity and that the crystallites were nanosized. There are no other characteristic peaks of impurities, such as CaO and other calcium phosphates. Crystallographic similarity of apatite samples come from the same hexagonal lattice structure of space group P63/m, with slight differences. The incorporation of fluoride ions into the apatite structure causes a decrease in the lattice parameter (a) (tab. 1). A significant in the lattice parameter (a) was observed in previous studies [16, 19]. Changes in the lattice parameter (a) are the result of differences in size, structures and physical properties of F^- (0.136 nm) and OH^- (0.14 nm) ions. Other ions, especially carbonate ions, influence the values of lattice parameters, which lead to a contraction in the a-axis dimension and expansion in the c-axis dimension. The incorporation of carbonate ions can also result in smaller crystals and amorphous products. According to FTIR analysis (fig. 2) carbonate ions are present in all samples.

EDS elemental analysis shows that all [Ca]/[P] ratios in the samples are similar to the amount of the starting material (tab. 2). According to the obtained results it can be assumed that fluoride ions are almost completely incorporated into the apatite structure. The existing differences can be related to the present traces of carbonate ions.

FTIR spectra of all apatite samples (fig. 2) displayed typical absorbance bands, which are in agreement with literature data [35]. The presence of weak bands at 870 cm^{-1} and 1430 cm^{-1}, indicate to a B-type substitution within some CO_3^2 groups in PO_4^3 sites of the apatite lattice. The intensity of these bands can indicate that a small amount of carbonate ions is incorporated into apatite samples. Natural fluoroapatites have a greater capacity to retain uranium and a bigger acidic solubility with an increase in the amount of carbonate ions [36, 37].

The morphology and size of apatite particles is influenced by many factors such as the type and concentration of the precursors, conditions of synthesis (pH, temperature) and optionally, a variety of organic substances such as surfactants, during the synthesis process. Silva *et al*. [38] reported that fluorapatite crystals are obtained from an aqueous solution in the course of 3 hours with a rod-like rectangular shape. Fluorhydroxyapatite nanorod particles with a relatively uniform rod-like morphology were obtained by a precipitation method in the precencepresence of a non-ionic surfactant [poly(oxyethylene)sorbitan monooleate] (Tween 80) and acetate ions [20]. The morphologies of synthesized apatite samples (fig. 3) are similar to the morphology found in hydroxyapatite powders prepared under microwave irradiation/iridation? in the presence of sodium lauryl ether sulfate or alkylbenzene sulfonate [39]. A comparison of the average particle size and the mean crystallite size (tab. 1), determined from the X-ray diffraction data, indicates a polycrystalline nature of the powder particles. According to the FESEM micrographs it can be concluded that the amount of fluoride ions does not significantly influence on the size and morphology of particles. Nanosized apatite displayed a fast and high sorption capacity of heavy metal ions [40, 41]. This is very important for rapid removal of heavy metal ions and the prevention of environmental threats.

The antimicrobial properties of synthesized fluorapatite powders as promising biomaterials for use in the reconstruction of bone defects would be of great relevance. In this study, antimicrobial activities of the

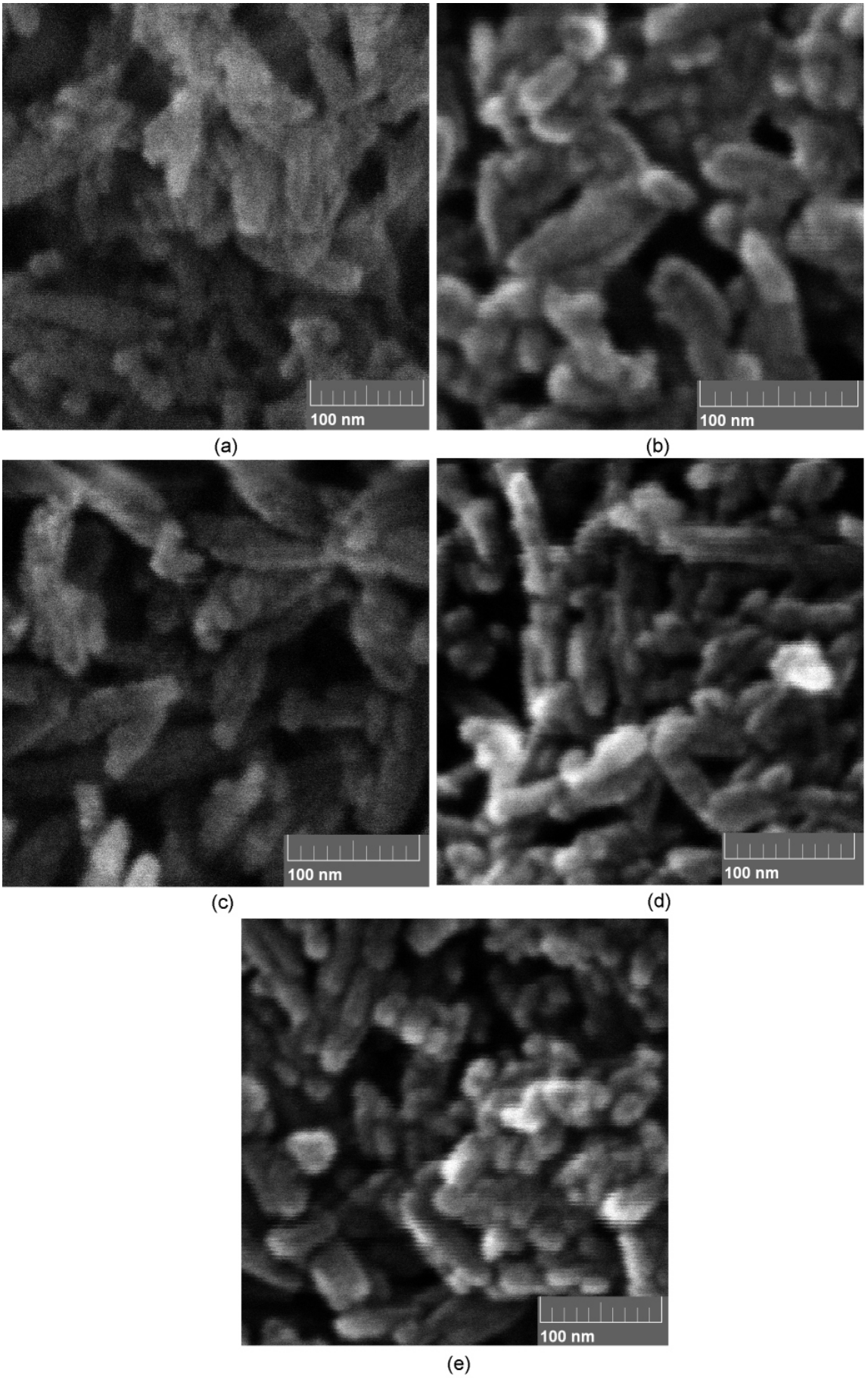

Figure 3. FESEM images of synthesized samples; HAP (a), FHAP1 (b), FHAP2 (c), FHAP3 (d), and FAP (e)

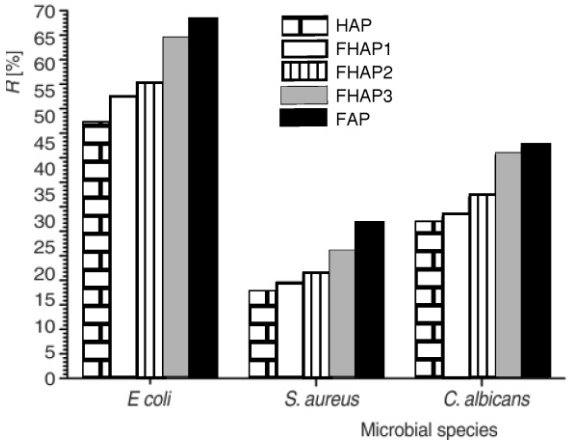

Figure 4. The comparative percentage of microbial reduction (R%) for *S. aureus*, *E. coli* and *C. albicans*, after the treatment with the synthesized apatite powders after 1 hour

fluorapatite samples were tested against *S. aureus*, *E. coli* and *C. albicans*, because those species have been involved in bone implants-related infections [42]. *S. aureus* appears as the main causative agent. Infections by *E. coli* and *C. albicans* as the main causes are rare.

According to the results of the antimicrobial assay (fig. 4), the hydroxyapatite sample showed a reduction in the viable cell number of investigated species as a result of their adhesion to the surface of the particles. Hydroxyapatite biomaterials do not have antimicrobial properties and microbes can colonize their surface. Fluoride ions decrease adhesion properties of some carcinogenic pathogen bacteria on a hydroxyapatite surface [43]. The percentage of microbial reduction after the treatment with the fluorapatite synthesized samples is higher and increases with the amount of fluoride (fig. 4). Among the tested microbial species, gram-negative bacteria *E. coli* are the most susceptible to the fluorapatite materials. The *E. coli* bacterium adheres more weakly to the surfaces of the fluorapatite cement than that on the natural enamel, indicating that fluorapatite cement could inhibit bacteria attachment and have antimicrobial properties [44]. Ge *et al*. [45] reported that fluorhydro- xyapatite coatings showed antibacterial activities against *Staphylococcus aureus* and *Escherichia coli* in phosphate buffered saline (pH 7.4). We previously, reported that the *K. pneumoniae* (gram-negative) bacteria showed greater sensitivity than *S. aureus* to pure and silver-doped fluorapatite materials [17]. *C. albicans* showed a slightly higher sensitivity than *S. aureus* toward fluorapatite materials (fig. 4). A previous study has shown that the use of fluoride proved to be a reducing agent for the growth and activity of *C. albicans* [46]. The mechanism of antimicrobial actions of fluoride ions is complex and incompletely understood. We suppose that the antimicrobial effect of fluorapatite samples is mainly based on fluoride ions released in the PBS solution. The fluoride ions can be released from fluorapatite particles in an alkaline medium by ion exchange with OH- ions [47].

CONCLUSION

Fluorapatite powders with different fluoride concentrations were synthesized in the micellar solution of the surfactant Brij 35 under microwave radiation and isothermal conditions, $T = 60$ ºC. The analysis of XRD, FTIR, and SEM showed that particles of fluorapatite samples are of nanosize and homogenous in composition. The synthesized fluorapatite samples showed antimicrobial activity against *S. aureus*, *E. coli* and *C. albicans*. The results of this study indicate that synthesized fluorapatite nanomaterials can be considered as a potential sorbent for toxic and radioactive heavy metals ions and antimicrobial biomaterials in orthopedics and dentistry.

ACKNOWLEDGEMENT

This work was supported by the Ministry of Education, Science and Technological Development of the Republic of Serbia (Project No. III 43009).

AUTHORS' CONTRIBUTIONS

The synthesis of fluorapatite materials was carried out by V. Dj. Stanić and B. K. Adnadjević. The physical and chemical characterization of synthesized materials was done by S. I. Dimitrijević, S. D. Dimović, M. N. Mitrić, B. B. Zmejkovski, and S. Smiljanić. All authors discussed the results and commented on the manuscript.

REFERENCES

[1] Lee, C. K., *et al*., The Removal of Heavy Metals Using Hydroxyapatite, *Environmental Engineering Research, 10* (2005) 5, pp. 205-212
[2] Stanić, V., Variation in Properties of Bioactive Glasses after Surface Modification, in: Clinical Applications of Biomaterials (ed. G. Kaur), Springer International Publishing, 2017, pp. 35-63
[3] Raičević, S., *et al*., Theoretical Stability Assessment of Uranyl Phosphates and Apatites: Selection of Amendments for *in situ* Remediation of Uranium, *Science of the Total Environment, 355* (2006), 1-3, pp. 13-24
[4] Viipsi, K., *et al*., Hydroxy- and Fluorapatite as Sorbents in Cd(II)-Zn(II) Multi-Component Solutions in the Absence/Presence of EDTA, *Journal of Hazardous Materials, 252- 253* (2013), May, pp. 91-98
[5] Kaludjerović-Radoičić, T., *et al*., Aqueous Pb Sorption by Synthetic and Natural Apatite: Kinetics, Equilibrium and Thermodynamic Studies, *Chemical Engineering Journal, 160* (2010), 2, pp. 503-510
[6] Dimović, S., *et al*., Speciation of ^{90}Sr and other Metal Cations in Artificially Contaminated Soils: the Influ-

ence of Bone Sorbent Addition, *Journal of Soils and Sediments, 13* (2013), 2, pp. 383-393
[7] Schindler, M., *et al*., Mobilization and Agglomeration of Uraninite Nanoparticles: A Nano-Mineralogical Study of Samples from the Matoush Uranium Ore Deposit, *American Mineralogist, 102* (2017), 9, pp. 1776-1787
[8] Eslami, H., *et al*., The Comparison of Powder Characteristics and Physicochemical, Mechanical and Biological Properties between Nanostructure Ceramics of Hydroxyapatite and Fluoridated Hydroxyapatite, *Materials Science and Engineering: C, 29* (2009), 4, pp. 1387-1398
[9] Ewing, R. C., *et al*., Phosphates as Nuclear Waste Forms, *Reviews in Mineralogy and Geochemistry, 48* (2002), 1, pp. 673-699
[10] Gerin, C., *et al*., Influence of Vacancy Damage on He Diffusion in Apatite, Investigated at Atomic to Mineralogical Scales, *Geochimica et Cosmochimica Acta 197* (2017), Jan., pp. 87-103
[11] Miro, S., *et al*., Effect of Composition on Helium Diffusion in Fluoroapatites Investigated with Nuclear Reaction Analysis, *Journal of Nuclear Materials, 355* (2006), 1-3, pp. 1-9
[12] Soulet, S., *et al*., Determination of the Defect Creation Mechanism in Fluorapatite, *Journal of Nuclear Materials, 289* (2001), 1-2, pp. 194-198
[13] Rakovan, J., *et al*., Structural Characterization of U(VI) in Apatite by X-Ray Absorption Spectroscopy, *Environmental Science & Technology, 36* (2002), 14, pp. 3114-3117
[14] Overgaard, S., *et al*., Resorption of Hydroxyapatite and Fluorapatite Coatings in Man, An Experimental Study in Trabecular Bone, *The Journal of Bone and Joint Surgery, 79* (1997), 4, pp. 654-659
[15] Cremet, L., *et al*., Orthopaedic-Implant Infections by *Escherichia Coli*: Molecular and Phenotypic Analysis of the Causative Strains, *Journal of Infection, 64* (2012), 2, pp. 169-175
[16] Stanić, V., *et al*., Synthesis of Fluorine Substituted Hydroxyapatite Nanopowders and Application of the Central Composite Design for Determination of Its Antimicrobial Effects, *Applied Surface Science, 290* (2014), Jan., pp. 346-352
[17] Stanić, V., *et al*., Synthesis, Structural Characterisation and Antibacterial Activity of Ag+-Doped Fluorapatite Nanomaterials Prepared by Neutralization Method, *Applied Surface Science, 337* (2015), May, pp. 72-80
[18] Stanić, V., *et al*., Synthesis, Characterization and Antimicrobial Activity of Copper and Zinc-Doped Hydroxyapatite Nanopowders, *Applied Surface Science, 256* (2010), 20, pp. 6083-6089
[19] Cavalli, M., *et al*., Hydroxy- and Fluorapatite Films on Ti Alloy Substrates: Solgel Preparation and Characterization, *Journal of Materials Science, 36* (2001), 13, pp. 3253-3260
[20] Zhang, H. G., *et al*., Surfactant-Assisted Preparation of Fluoride-Substituted Hydroxyapatite Nanorods, *Materials Letters, 59* (2005), 24-25, pp. 3054-3058
[21] Fahami, A., *et al*., Mechanochemical Behavior of $CaCO_3$-P_2O_5-CaF_2 System to Produce Carbonated Fluorapatite Nanopowder, *Ceramics International, 40* (2014), 9, pp. 14939-14946
[22] Rameshbabu, N., *et al*., Synthesis of Nanocrystalline Fluorinated Hydroxyapatite by Microwave Processing and Its *in vitro* Dissolution Study, *Bulletin of Materials Science, 29* (2006), 6, pp. 611-615
[23] Loher, S., *et al*., Fluoro-Apatite and Calcium Phosphate Nanoparticles by Flame Synthesis, *Chemistry of Materials, 17* (2005), 1, pp. 36-42
[24] Adnadjević, B., *et al*., A Novel Approach to the Explanation the Effect of Microwave Heating on Isothermal Kinetic of Crosslinking Polymerization of Acrylic Acid, *Russian Journal of Physical Chemistry A, 87* (2013), 13, pp. 2115-2120
[25] Adnadjević, B., *et al*., Kinetics of the Apparent Isothermal and Non-Isothermal Crystallization of the a-Fe Phase within the Amorphous $Fe_{81}B_{13}Si_4C_2$ alloy, *Journal of Physics and Chemistry of Solids, 71* (2010), 7, pp. 927-934
[26] Gopi, D., *et al*., Influence of Surfactant Concentration on Nanohydroxyapatite Growth, *Bulletin of Materials Science, 36* (2013), 5, pp. 799-805
[27] Arami, H., *et al*., Rapid Formation of Hydroxyapatite Nanostrips via Microwave Irradiation, *Journal of Alloys and Compounds, 469* (2009), 1-2, pp. 391-394
[28] Kovačević, A., *et al*., Uncertainty Evaluation of the Conducted Emission Measurements, *Nucl Technol Radiat, 28* (2013), 2, pp. 182-190
[29] Kovačević, A., *et al*., The Combined Method for Uncertainty Evaluation in Electromagnetic Radiation Measurement, *Nucl Technol Radiat, 29* (2014), 4, pp. 279-284
[30] Kovačević, A. Stanković, K., The Numerical Method for the Coverage Interval Determination in the Conducted Emission Measurements, *Measurement, 91* (2016), Sept., pp. 221-227
[31] Stanić, V., *et al*., Synthesis of Antimicrobial Monophase Silver Doped Hydroxyapatite Nanopowders for Bone Tissue Engineering, *Applied Surface Science, 257* (2011), 9, pp. 4510-4518
[32] Ross, S., *et al*., A New Method for the Determination of Critical Micelle Concentrations of Un-Ionized Association Colloids in Aqueous or in Non-Aqueous Solution, *The Journal of Physical Chemistry, 63* (1959), 10, pp. 1671-1674
[33] Sharma, B., *et al*., Thermodynamics of Micellization of a Nonionic Surfactant: Brij 35 in Aquo-Sucrose Solution, *Journal of Colloid and Interface Science, 129* (1989), 1, pp. 139-144
[34] Schwarzenbacher, R., *et al*., Characterization of the Nanostructures in Liquid Crystalline Mesophases Present in the Ternary System Brij-35/dibutyl ether/H_2O by Small- and Wide-Angle X-Ray Scattering, *The Journal of Physical Chemistry B, 102* (1998), 45, pp. 9161-9167
[35] Rehman, I., *et al*., Characterization of Hydroxyapatite and Carbonated Apatite by Photo Acoustic FTIR Spectroscopy, *Journal of Materials Science: Materials in Medicine, 8* (1997), 1, pp. 1-4
[36] Clarke, R. S., *et al*., Determination of the Oxidation State of Uranium in Apatite and Phosphorite Deposits, *Geochimica et Cosmochimica Acta, 13* (1958), 2-3, pp. 127-142
[37] Veeh, H. H., *et al*., Accumulation of Uranium in Sediments and Phosphorites on the South West African Shelf, *Marine Chemistry, 2* (1974), 3, pp. 189-202
[38] Silva, G. W. C., *et al*., Micro-Structural Characterization of Precipitation-Synthesized Fluorapatite Nano-Material by Transmission Electron Microscopy Using Different Sample Preparation Techniques, *Micron, 39* (2008), 3, pp. 269-274
[39] Amer, W., *et al*., Microwave-Assisted Synthesis of Mesoporous Nano-Hydroxyapatite Using Surfactant Templates, *Cryst Eng Comm., 16* (2014), 4, pp. 543-549
[40] Ma, B., *et al*., Adsorptive Removal of Co and Sr Ions from Aqueous Solution by Synthetic Hydroxyapatite Nanoparticles, *Separation Science and Technology, 45* (2010), 4, pp. 453-462
[41] Feng, Y., *et al*., Adsorption of Cd (II) and Zn (II) from Aqueous Solutions Using Magnetic Hydroxyapatite

Nanoparticles as Adsorbents, *Chemical Engineering Journal, 162* (2010), 2, pp. 487-494
[42] Campoccia, D., *et al*., The Significance of Infection Related to Orthopedic Devices and Issues of Antibiotic Resistance, *Biomaterials, 27* (2006), 11, pp. 2331-2339
[43] Loskill, P., *et al*., Reduced Adhesion of Oral Bacteria on Hydroxyapatite by Fluoride Treatment, *Langmuir, 29* (2013), 18, pp. 5528-5533
[44] Wei, J., *et al*., Development of Fluorapatite Cement for Dental Enamel Defects Repair, *Journal of Materials Science: Materials in Medicine, 22* (2011), 6, pp. 1607-1614
[45] Ge, X., *et al*., Antibacterial Coatings of fluori-Dated Hydroxyapatite for Percutaneous Implants, *Journal of Biomedical Materials Research Part A, 95* (2010), 2, pp. 588-599
[46] Flisfisch, S., *et al*., Effects of fluorides on *Candida Albicans*, *Oral Diseases, 14* (2008), 4, pp. 296-301
[47] Bengtsson, A., *et al*., Phase Transformations, Ion-Exchange, Adsorption, and Dissolution Processes in Aquatic Fluorapatite Systems, *Langmuir, 25* (2009), 4, pp. 2355-2362

Received on December 5, 2017
Accepted on February 12, 2018

Војислав Ђ. СТАНИЋ, Боривој К. АДНАЂЕВИЋ, Сузана И. ДИМИТРИЈЕВИЋ, Славко Д. ДИМОВИЋ, Миодраг Н. МИТРИЋ, Бојана Б. ЗМЕЈКОВСКИ, Славко СМИЉАНИЋ

СИНТЕЗА ФЛУОРОПАТИТНИХ НАНОПРАХОВА ПОМОЋУ МИКРОТАЛАСНЕ МЕТОДЕ У ПРИСУСТВУ ТЕНЗИДА ПОД ИЗОТЕРМАЛНИМ УСЛОВИМА

Флуороапатитни нанопрахови са различитим количинам флуоридних јона направљени су помоћу микроталасне методе у присуству тензида под изотермалним условима. Мицеларни раствор полиоксиетилен (23) лаурил етера коришћен је као регулатор нуклеације и раста кристала. Карактеризационе студије: рендгеноструктурна анализа, емисиона скенирајућа електронска микроскопија и Фурије-трансформисани инфрацрвени спектри, показале су да кристали имају апатитну структуру и да су честице свих узорака нановеличине, са средњом дужином око 50 nm и око 15-25 nm у пречнику. Антимикробне студије показале су да синтетисани флуороапатитни нанопрахови испољавају активност против тестираних патогена: *Escherichia coli, Staphylococcus aureus* и *Candida albicans.* Активност се повећала са количином флуоридних јона. Синтетисани флуороапатитни нанопрахови су обећавајући материјали у заштити животне средине и у медицини за ортопедске и зубне реставрације.

Кључне речи: флуороапатит, микроталасна обрада, нанопрах, заштита животне средине